

Grid Spatial Understanding: A Dataset for Textual Spatial Reasoning over Grids, Embodied Settings, and Coordinate Structures

Risham Sidhu, Julia Hockenmaier
University of Illinois at Urbana-Champaign

Abstract

We introduce GSU, a text-only grid dataset to evaluate the spatial reasoning capabilities of LLMs over 3 core tasks: navigation, object localization, and structure composition. By forgoing visual inputs, isolating spatial reasoning from perception, we show that while most models grasp basic grid concepts, they struggle with frames of reference relative to an embodied agent and identifying 3D shapes from coordinate lists. We also find that exposure to a visual modality does not provide a generalizable understanding of 3D space that VLMs are able to utilize for these tasks. Finally, we show that while the very latest frontier models can solve the provided tasks (though harder variants may still stump them), fully fine-tuning a small LM or LORA fine-tuning a small LLM show potential to match frontier model performance, suggesting an avenue for specialized embodied agents.

1 Introduction

With the advent of more powerful LLMs, their applications have broadened from text generation to complex problems ranging from advanced mathematical reasoning to multimodal agents. Many of these tasks require the ability to reason about space, whether to solve geometry problems (Zhao et al., 2025; Gao et al., 2025) or to understand verbal commands about their surroundings as an embodied agent (Zhang et al., 2024; Feng et al., 2025), to complete tasks while interacting with objects in complex environments (Padmakumar et al., 2021; Shridhar et al., 2020), to describe visual scenes (Fu et al., 2024a), or to reason over 2- and 3-D images (Cheng et al., 2024; Chen et al., 2024).

Approaches to such tasks incorporate additional modalities through vision encoders, projections of point cloud data, or more specialized representations, but using these effectively necessitates updates to base LLM architecture or additional training. Furthermore, even with such additions, it is

unclear if fundamentally non-physical models that have been trained primarily on unpaired text can truly understand 3D space. Despite recent advances on various spatial reasoning tasks, the internal reasoning processes of LLMs, VLMs, and variations thereof are often not interpretable, meaning that merely measuring performance is distinct from evaluating understanding. And even when performance is strong, further investigations into how additional modalities, like vision, are used in spatial tasks reveal that multi-modal LLMs receive little additional information from images when provided with rich text representations (Wang et al., 2024a).

In that case, textual descriptions of physical space may serve as a convenient proxy for complex visual inputs when evaluating spatial reasoning. By removing visual perceptions, they offer a controlled method of probing whether LLMs possess robust internal representations of space, and if such representations can be manipulated with textual descriptions alone. Given that grids are an established representation for 3D space, they are a natural choice to express 3D layouts and movements.

In this work, we present GSU, a dataset composed of 3 simple text-only grid spatial reasoning tasks aimed at applications in embodied domains, to serve as a diagnostic for the inherent spatial reasoning abilities of existing models and identify where further work is needed to induce the spatial capabilities embodied agents require.

- The **Navigation** Task requires instruction generation or following on 2D and 3D grids with two potential spatial frames of reference: *Cardinal* (i.e. fixed), testing recognition of 1D directional differences in coordinates, and *Ego-centric* (i.e. moving with an embodied agent), testing understanding of rotating/updating spatial reference frames.
- The **Object Localization** task asks where tar-

gets are relative to a viewer (*Egocentric*), testing 2D and 3D direction differences between coordinates, or relative to a separate spatial reference (*Allocentric*), testing spatial reference in collaborative settings.

- The **Structure Composition** task needs models to translate sets of coordinates into basic shapes (e.g. rows, columns, cubes), testing ability to link coordinates to real-world shapes and process large numbers of coordinates.

2 The GSU Dataset

We now expand on each of these relatively simple spatial tasks and the specific facets of textual coordinate reasoning they test. For more details on generation and dataset statistics, please refer to Appendix A.

2.1 The Navigation Task

The first task measures models' understanding of textual coordinates as a representation of physical space. In this task, models must correlate natural language directions (i.e. "left", "down", "backward") with grid traversals across coordinates differing in 1 dimension at a time, i.e. equating moving from (0, 0) to (2, 0), to (2, 1) with moving "right 2" and "forward 1".

2.1.1 Instructor vs. Follower

VLN tasks are generally a conversation between two counterparts: an instructor and a follower. While the instructor is often a person and the follower an agent, this is not necessarily always the case (e.g. a collaborative system with multiple agents, Narayan-Chen et al. (2019)'s MDC Architect task, voice assistants, etc). Models should thus be proficient in both directions of this mapping between verbal spatial directions and coordinate traversals.

In the *Follower* setting, models receive a set of natural language instructions explaining how to traverse the grid (e.g. "move right 2 steps and then forward 1") and must output a coordinate reflecting their final location (e.g. (2, 1)). Whereas in the *Instructor* setting, models receive a grid traversal expressed as a series of intermediate coordinates (e.g. (0, 0), (2, 0), (2, 1)) and must output the natural language instructions that correlate to that path (e.g. "move right 2 and forward 1").

2.1.2 Spatial Frames of Reference

We consider two frames of reference for the spatial directions of the grid. In the *Cardinal* setting, the spatial directions are fixed to the axes of the grid and never change, i.e. to move forward always means to increase the y value, while to move left always means to decrease the x value. While many grid based tasks use this fixed perspective of spatial relations (e.g. Aghzal et al. (2025)), it does not transfer well to practical collaborative settings where an embodied agent or a human it is instructing have their own frame of reference that may not align with a fixed grid.

The *Egocentric* formulation aligns spatial directions with the perspective of an embodied subject navigating the grid, orienting the spatial directions with their body, and so rotating where they are relative to the fixed axes of the grid. For example, in the *Egocentric* setting to go right 2 steps and then forward 1 step would first entail turning to the right (90° clockwise to face +X) and moving two steps in that direction. Then, moving 1 step forward would no longer mean increasing the y value, but rather continuing forward in our current heading/direction of travel, i.e. increasing our x value. This would be equivalent to moving 2 steps right and then 1 more step right in the *Cardinal* setting. (See Figure 1 for a visualization.)

Additionally, we include a simpler form of the *Egocentric Instructor* setting, *Card2Ego*. Rather than going from coordinates to egocentric spatial directions, *Card2Ego* asks models to translate cardinal spatial directions (North/South/East/West) into egocentric spatial directions (left/right/forward/backward).

2.2 The Object Localization Task

The object localization task focuses on understanding how grid coordinates are situated spatially relative to one another. Specifically, given a viewer at a location and with a particular heading, we ask models to determine where a target at a randomly generated coordinate is relative to that viewer (*Egocentric*) or where it is relative to a reference at another randomly generated coordinate (*Allocentric*). In the former, models are expected to reply with something to the effect of the object is "to my right" and in the latter with the target is "to the right of" the reference.

In this task, we vary the heading of the viewer (i.e. which axis they are facing parallel to), the

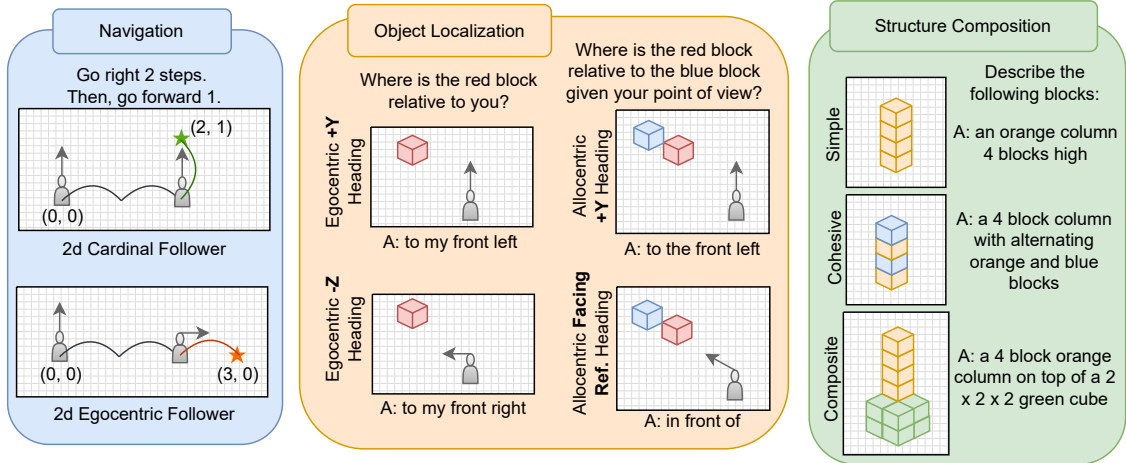


Figure 1: The GSU Dataset tasks and settings visualized for clarity (note that the models do NOT receive these visuals and instead receive a textual version of the environment shown in Appendix E). The grey arrows indicate the heading, i.e. direction that the embodied agent is facing. In the Navigation task, they remain aligned with +Y in the *Cardinal* setting and rotate to reflect the last direction of travel in the *Egocentric* setting, which affects the direction of the second step and the final coordinates. For the Object Localization task, we show how different headings affect the spatial relations between the target and the reference. For the Structure Composition task, we show the 3 structure categories that models may be asked to describe.

distance between the target and the reference (are they adjacent to each other or further away), and add distractors (see Appendix A for more).

2.3 The Structure Composition Task

The final task explores a model’s ability to understand how blocks/voxels can be composed into larger overall structures. Not only does it require an understanding of how coordinates relate to real space, but also a knowledge of basic shapes/forms (e.g. a series of blocks that differ only in their z-dimension are stacked vertically and thus a column) and the ability to compose large lists of coordinates into meaningful information.

2.3.1 Composition Types

In the most basic setting, *Simple*, the selected coordinates form one structure of a single color and the model must interpret what 3D shape their arrangement forms (e.g. "an orange row 5 blocks long" or "a 3 x 3 x 3 green cube"). Slightly more complicated is the *Cohesive* setting where multiple colors of blocks form a single structure and the challenge is to understand how those colors interact with the structure (e.g. compare "a row with alternating orange and blue blocks" and "a row with an orange left half and a blue right half"). Finally, the *Composite* setting places 3 single-colored shapes adjacent to each other, asking the model to identify the 3 shapes, their colors, and where they

are relative to each other.

3 Experiments

To explore grid spatial understanding over a variety of model families, sizes, and types, we tested 5 broad categories of models. First, we tested small text-only models: Mistral-7b (Jiang et al. (2023)’s Mistral-7b-Instruct-v0.3), Llama-8b (Grattafiori et al. (2024)’s Llama3.1-8b-Instruct), and Qwen-7b (Yang et al. (2024); Team (2024)’s Qwen2.5-7b-Instruct). Additionally, we prompted their most similarly sized Vision-Language counterparts to see if exposure to a visual modality (even if it is not being utilized) can induce further spatial understanding: Pixtral-12b (Agrawal et al., 2024), LlamaVL-11b (Grattafiori et al. (2024)’s Llama3.2-11b-Vision-Instruct), and QwenVL-7b (Team (2025a); Bai et al. (2023); Wang et al. (2024b)’s Qwen2.5-VL-7B-Instruct). We also evaluated larger models, as they are known to be more powerful than their smaller counterparts: GPT-OSS20b (OpenAI, 2025), Qwen32b and QwenVL-32b ((Team, 2025b)’s 32b Instruct variants), Olmo-32b (Olmo et al., 2025), Qwen-72b (Yang et al. (2024); Team (2024)’s Qwen2.5-72B-Instruct). Finally, to consider frontier models, we choose GPT-4o (OpenAI et al., 2024) and Gemini-3-Pro (Team et al., 2025) accessed as Gemini-3.1-Pro-Preview, and to compare overall performance to a much

smaller model (<1B params) that can be fully fine-tuned, we fully train FlanT5-large (Chung et al., 2022).

For the purposes of prompting we generate test sets for each task of size 100 and for training we generate another of size 3000 (we did not see marked improvement in training by increasing the dataset size beyond this, see Appendix B.1 for more details). The *Navigation* and *Object Localization* experiments in Table 1 are 1-shot prompting with a handwritten example that includes the full reasoning needed to generate an answer. For the *Structure Composition* task in Table 1 the experiments are 3-shot prompting with synthetic examples and no reasoning. These settings were chosen based on performance (see Tables 9 and 15 in the Appendix), though we explain the difference in behavior as: the *Navigation* and *Object Localization* tasks require some amount of reasoning to work out headings and spatial relations, thus benefit more from one dense example that gives an example reasoning trace, while the *Structure Composition* task needs no explicit reasoning (just the ability to compose coordinates together) and thus benefits from a larger quantity of examples.

3.1 Metrics

3.1.1 Navigation Metrics

For the *Follower* task, we evaluate the accuracy of the predicted final coordinates as an exact match (i.e. there is no partial credit for getting the x-coordinate correct if the y-coordinate is incorrect) and for the *Instructor* we measure the exact match accuracy of the generated instruction chain (i.e. every step must be correct for the model to get credit). For a less exacting metric, we computed the distance between the true final coordinates and: the generated coordinates in *Follower* and the final coordinates obtained by executing the generated instruction chain in *Instructor*. As they tracked closely with the accuracies they are reported in see Appendix Table 8.

3.1.2 Object Localization Metrics

To measure model performance on the Object Localization tasks, we compute, O_s , the term overlap of the spatial relations in the predicted text, p , and the ground truth text, g .

$$O_s = \frac{E_r(p) \cap E_r(g)}{E_r(p) \cup E_r(g)} * 100$$

where the function E_r creates a set from each individual spatial relation extracted from the text. Essentially, it takes how many of the spatial terms in the generated sequence p are correct and divides this by the size of the set union of all correct spatial terms in the ground truth, g , and all generated spatial terms in p . For example, if the correct spatial relations, $E_r(g)$ are {"front", "left"}, the model may score a 0 ($E_r(p) = {"right"}$), a 33.33 ($E_r(p) = {"front", "above"}$), a 50 ($E_r(p) = {"front"}$), a 66.67 ($E_r(p) = {"above", "front", "left"}$), or a 100 ($E_r(p) = {"front", "left"}$). This penalizes models for predicting incorrect terms, while reducing this penalty for harder examples with more spatial relations to account for.

3.1.3 Structure Composition Metrics

We continue to use the spatial overlap metric, O_s , described in 3.1.2 and add three additional overlap metrics: O_c , which measures the overlap of the color terms, O_n , which measures numerical overlap, and O_f , which measures the overlap of the structure formation terms. For O_n , we use the same simple overlap as O_s , dividing how many correct numbers were generated by the size of the union of all the ground truth numbers and all generated numbers. However, unlike the Object Localization task, we have the opportunity for multiple structures to have the same color in the *Composite* setting, so the formulation for O_c is slightly different:

$$O_c = \frac{\sum_{colors} \min(C_c(p, color), C_c(g, color))}{\sum_{colors} \max(C_c(p, color), C_c(g, color))} * 100$$

where $C_c(text, term)$ counts the occurrence of $term$ or its synonyms in the text $text$. Thus, a generation that only identifies one yellow shape in a structure with 2 yellow sub-structures is penalized, as is a model that predicts 2 yellow shapes in a structure with just 1.

O_f follows the same base logic as O_c , but with more varied synonyms checked in C_f and partial credit afforded for predicting similar but not correct shapes. E.g. rather than getting no credit for predicting "a blue row on the ground" for a blue column, we award partial credit based on how similar the shapes are. (see Appendix A.1)

4 Results and Discussion

In this section we will briefly cover the 3 GSU task results shown in Table 1 before covering broader trends: manipulating spatial reference frames (4.1),

	Navigation					Object Localization		Structure Composition			
	Follower 2D		Instructor			Ego- centric	Allo- centric	O_s	O_c	O_f	O_n
	3D	Card.	Ego.	Card2Ego							
Mistral-7b	0.30	0.38	0.59	0.15	0.27	30.32	46.50	49.75	72.60	30.21	20.01
Pixtral	0.33	0.50	0.87	0.26	0.35	40.83	48.18	66.25	87.68	42.16	55.43
Llama-8b	0.33	0.47	0.69	0.06	0.09	46.17	50.18	62.04	86.69	22.70	37.75
LlamaVL-11b	0.32	0.47	0.74	0.14	0.28	48.40	48.08	64.48	86.58	44.44	44.05
Qwen-7b	0.09	0.19	0.76	0.21	0.36	52.81	54.78	54.58	85.43	28.57	42.97
QwenVL-7b	0.29	0.21	0.44	0.21	0.30	48.67	44.95	54.58	85.43	33.46	43.57
GPT-oss-20b	0.15	0.16	0.26	0.10	0.58	59.90	45.46	62.88	57.11	43.60	48.47
Olmo-32b	0.34	0.40	0.48	0.14	0.62	85.98	54.17	65.33	91.97	48.60	54.60
Qwen-32b	0.37	0.32	0.58	0.21	0.60	33.95	27.25	69.10	87.98	42.76	66.65
QwenVL-32b	0.38	0.52	0.12	0.17	0.64	68.03	50.80	67.40	93.62	55.09	68.22
Llama-70b	0.41	0.65	0.26	0.09	0.1	75.23	22.14	62.17	86.88	47.80	50.95
Qwen-72b	0.49	0.75	1.0	0.47	0.53	79.53	53.83	70.67	88.11	42.81	69.23
GPT-4o	0.71	0.84	0.89	0.67	0.93	96.00	65.50	69.20	88.63	52.85	82.28
Gemini-3-Pro	1.0	1.0	1.0	1.0	1.0	100	93.0	79.67	97.83	87.45	90.68
FlanT5	0.80	0.82	0.99	0.95	1.0	19.5	94.5	99	96.17	88.83	97.07
Llama-8b	0.82	0.96	0.57	0.61	0.99	87.23	81.83	99.33	100	93.42	96.33

Table 1: 3 GSU task results across 3 model categories (prompted LLMs and VLMs, prompted frontier models, and fine-tuned models) with best scores from each bolded. *Navigation* results are accuracies: final coordinate accuracies for the *Egocentric Follower* and instruction sequence accuracy for the *2D Instructor*, while *OL* and *SC* results are term overlaps: spatial O_s , color O_c , shape/form O_f , and numerical O_n . Other settings in Appendix D.

effects of a visual modality (4.2), frontier model capability (4.3), and improving small LLMs (4.4).

Navigation: We see that the *Instructor* setting provides a greater challenge for prompted models, with the *2D Egocentric Instructor* in Table 1 generally showing significant drops compared to the *2d Egocentric Follower*. The *Egocentric* variant is also more difficult as we see in the accuracy difference between the *Cardinal* and *Egocentric Instructor*. (These patterns hold over all settings, see Appendix D for more details.)

Object Localization: In the *Egocentric* case we see that smaller models receive scores below 50, consistent with further analysis that they often generate spatial relations for axes in which the target and reference do not differ. Larger models adeptly identify the reasoning structure from the example and isolate which axes coordinates differ on, but then fail to assign the correct spatial relation.

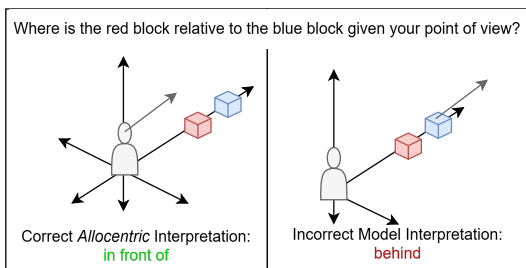


Figure 2: *Allocentric* front/back flipping

Most models perform worse on the *Allocentric* variant, suggesting that models struggle to reason about how two grid coordinates are situated relative to each other from the agent perspective (a third coordinate). Those that performed better were likely benefiting from the consistent $+Y$ heading in the *Allocentric* setting rather than displaying a particular strength at the task itself. Notably, many models flip the forward and backward directions as their main source of error in this variant. If the target is between the viewer and the reference, many LLMs describe it as "behind" the reference, rather than "in front" of the reference, as if the reference is the viewer. (see Figure 2).

Structure Composition: In this task, we see similar spatial (O_s) performance to the *OL* task, with models often opting to not describe where shapes were relative to each other unless they are certain, and strong color (O_c) performance, with mistakes due to omissions rather than hallucinations. The numerical overlap (O_n) errors are caused by models miscounting or due to unconventional ways of breaking up structure descriptions: e.g. rather than describing a $3 \times 3 \times 8$ rectangular prism with those dimensions, one generation describes it as a group of 10 columns each 7 blocks high. While this could describe a similar shape (though it could also be a 7×10 plane) and certainly accounts for a similar number of blocks, it

receives no credit for either metric.

Overall, the generated descriptions are comprehensible and seem reasonable when viewed independently of the ground truth. In 0-shot settings (Appendix Table 14), models generated vague answers, e.g.: "*a continuous layer of blocks*" rather than concrete shapes, e.g. "*a 4 x 7 rectangle*". This behavior extends into the few-shot setting, with numerous productions of "structure", "formation", and "platform" modified by rich adjectives, such as "*a large, flat, expansive structure*". Models also flatten 3D shapes, outputting "square" for cube and "rectangle" for rectangular prisms. Other times they name a shape incorrectly, but still display insight into the formed structure, such as calling a $2 \times 2 \times 8$ rectangular prism a "*cube with height 8 and width 2*" (fundamentally not a cube, but still displaying spatial understanding that is rewarded by the O_n metric instead). A notable threshold that stronger models cross is distinguishing rows and columns: stronger models identify which axes the blocks differ on and rarely conflate the two, instead mixing up cubes with rectangular prisms or vertical rectangular prisms with columns. Generally, weaker models also omit reasoning for the shapes they produce, while stronger models like Gemini explain how the coordinate ranges influence its productions, which is reflected in its scores.

4.1 Manipulating Spatial Reference Frames

The reasoning traces of the models corroborate the score disparity between *Cardinal* and *Egocentric Navigation* tasks in Tables 1 and 10. In the former setting, most models output neat, contained logic with only occasional errors, while in the latter, models fail to keep the X and Y axes oriented consistently, leading to generations such as "*we are facing $-Y$ with $+Y$ to our right*" and "*we turned towards $+X$, so we're facing $-X$* ". Larger models, though less likely to make these mistakes, calculate updated headings after a turn and then "forget" to use them in the next step, outputting logic and final coordinates consistent with the fixed grids of the *Cardinal* setting.

In the *Egocentric Object Localization* tasks, this aversion to non-standard spatial reference frames manifests as non sequitur logic where the model establishes the correct heading in the premise but completes the generation with an incorrect deduction. These deductions are generally consistent with the standard $+Y$ heading, e.g. while facing $-Y$: "*I know that $-X$ is to my right* [correct

premise] "*so x values smaller than me are to my left*" [incorrect deduction consistent with a $+Y$ heading instead]. The spatial term overlap, O_s is also higher for the $+Y$ heading than any other (Appendix Table 12). This phenomenon might also explain poor performance on the *Allocentric* variant in Table 1, particularly the forward/backing flipping described in Figure 2, as models struggle to reconcile how two frames of reference interact with each other.

We suspect that the inability to correctly reorient the spatial reference frame is due in part to exposure to the standard Cartesian orientation in pre-training and in part due to the complexity of updating it. This is supported by the Table 1 *Navigation Card2Ego* results, where any mathematical reasoning about textual grid coordinates is completely absent, replaced by converting Cardinal directions into relative ones. LLMs have an easier time with *Card2Ego* than the *Egocentric Instructor* but still fall short, showing that, in addition to struggling with grid coordinates, LLMs consistently struggle with the concept of rotating spatial frames of reference outside of explicit grids too.

4.2 Effects of the Visual Modality

As shown by the 4 VLMs shown in light blue under their LLM counterparts in Table 1, there is no clear correlation between exposure to a visual modality and improved reasoning over textual coordinate grids, especially in the smaller models. For example, on the *Navigation* tasks, Pixtral outperforms Mistral, while Qwen outperforms Qwen-VL, and both Llama models perform similarly, though perhaps the consistent pattern within each model family can be attributed to how vision is integrated into their respective VLMs. In some of the tasks (e.g. *Object Localization*), we see that Qwen-32B-VL outperformed Qwen-32B and in others (i.e. *Structure Composition*), all VLMs outperform their LLM counterparts: these patterns may suggest that VLMs need at least a certain LLM size before being able to utilize information gained from interacting with a textual modality or that they confer more benefits when reasoning over coordinate structures rather than spacial relations.

4.3 Frontier Capabilities

As expected, the frontier models outperform smaller LLMs, though notably Qwen-72b is able to match their performance on some tasks and even outperform GPT-4o. While proficient in the

Cardinal setting, GPT-4o struggles to keep track of spatial references in the *Egocentric* one, incorrectly computing the current heading or forgetting to act according to an updated heading, especially in longer sequences (see Appendix Table 11). For example, GPT-4o generates that it was "currently facing $-X$, but need[ed] to move right [and moving] right means turning 90 degrees clockwise so that's $+X$ ". This final heading should have been $+Y$, a rotation that GPT handles successfully in shorter sequences. However, a right turn leading to facing $+X$ is consistent with the fixed *Cardinal* frame of reference, which the model seems to default to, even in the midst of egocentric-compliant reasoning.

The latest Gemini model solves multiple tasks completely, even harder variants of the tasks such as arbitrarily long navigation sequences with non-integer step lengths or non-axis aligned turns. It also performs surprisingly well on distinguishing independent block structures from scrambled lists of individual blocks. Given this, we must acknowledge that Gemini-3-Pro has spatial understanding when it comes to spatial frames of reference relative to an embodied agent and composing blocks into larger structures. At the very least, it must have been exposed to similar problems, perhaps in a mathematical context.

However, that is not to say there is no room for improvement within the domain of textual grid based tasks. We further prompt Gemini on a task combining each of the 3 task categories: an egocentric agent must follow navigation instructions and then answer where two block-based structures are relative to each other (see E.6). This requires the model to: (a) successfully complete egocentric navigation and identify its final heading, (b) distinguish the target and reference structures from distractor objects, all presented as a single list of blocks, and (c) identify where the target is relative to the reference. Here, we find that even Gemini fell short, with a final spatial overlap O_s of 0.62: it sometimes mixes up similar shapes, struggles with the forward/backward issue, and makes slight errors in relative spatial relations given the 3D nature of block structures.

4.4 Improving Small LLMs

We anticipate that more frontier models will develop enough spatial reasoning to solve the base tasks, and eventually the harder variants as well. However, the simplicity of GSU and the subsequent

gap between it and real-world scenarios, motivates us to want stronger small LLMs. To that end, we train our worst performing small LLM (Llama-8b) with LORA to elicit an underlying spatial understanding. Initial experiments reduced performance on the *Navigation* task and so to better match natural LLM outputs, we generate synthetic reasoning traces to accompany the ground truth answers for the *Navigation* and *Object Localization* tasks. (This also matched our prompting findings in Appendix Tables 9 and 15 that showed a single example with strong reasoning improved performance more than multiple examples without reasoning.) As we show in Table 1, with these reasoning traces, Llama-8b shows improved performance on the *Object Localization* tasks (the reasoning traces offered slight LORA performance boosts). It also more than doubles its performance on the *Navigation Follower* tasks after LORA, outperforming GPT-4o and almost matching Gemini. For the *Navigation Instructor* tasks, improvement is even more drastic for the *Egocentric* and *Card2Ego* versions it initially struggled with, increasing performance tenfold. With this, we show that textual spatial reasoning is not out of reach for smaller models and their potential to match frontier models.

We also note that fully finetuning a small model like FlanT5 (<1B params) is sufficient to outperform many LLMs and match performance with some frontier models, especially on sequence generation tasks like *Navigation Instructor* (Table 1). This highlights how simple the tasks should be to solve: a lightweight model a fraction of the size is better at identifying shapes from coordinate lists of blocks, where those shapes are relative to each other, and generating instructions for grid navigation.

5 Related Works

Spatial Reasoning Instead of text, physical information is generally conveyed to LLMs via images, either from external POVs like observing scenes from above (Li et al., 2024a) or from the perspective of embodied agents for applications like VLN, and pointcloud embeddings (Hong et al., 2023). However, even after integrating additional modalities and achieving strong performance on many visual tasks, VLMs could not understand or reason about physical space as capably as humans, struggling with spatial VQA, particularly object orientations in images (Liao et al., 2024; Liu et al.,

2023) and mental transformations like rotations (Stogiannidis et al., 2025). They fall well short of human performance localizing objects within scenes and reasoning about object dimensions (Majumdar et al., 2024). Some have proposed addressing these spatial reasoning shortcomings with training datasets that align 2D images with textual tasks about the orientation of, distance between, and location of nodes Tang et al. (2025), while others have questioned what VLMs are actually perceiving in images and found that they perform just as well with rich text descriptions instead of input images (Wang et al., 2024a; Fu et al., 2024b).

Combined with the difficulty of isolating spatial performance from visual perception, this motivates text-only spatial reasoning to evaluate the "mental" models LLMs have of space. Some use graphs, exploring graph traversals in which LLMs hallucinate nodes, take suboptimal paths, and deteriorate on denser graphs (Momennejad et al., 2023) or describing spatial relations between graph nodes using multihop reasoning over intermediary nodes (Shi et al., 2022; Li et al., 2024b). Others are nominally set in grids, such as Yamada et al. (2024) which explores 2D grid navigation but only on closed loop paths using relative descriptions of positions and Mayer et al. (2025), which proposes a visual puzzle game on grid, but compares visual representation to a chess-style notation for the textual representation. Few consider coordinates for text-only spatial reasoning tasks (a notable exception being Aghzal et al. (2025)'s evaluation of LLM path planning through obstacles on fixed 2D grids) despite coordinate grids being a standard for representing space and likely plentiful in LLM pretraining data.

One context in which LLMs may have encountered coordinates or reasoning about them is math problems. While most coordinates in such problems are paired with text and the associated reasoning is unrelated to spatial relations, the success in mathematical reasoning (Shao et al., 2024; Ahn et al., 2024; Wang et al., 2025) and a variety of math datasets (Hendrycks et al., 2021; Chen et al., 2022) suggests that coordinate spatial reasoning is not outside the realm of LLM abilities.

Applications GSU distills the spatial reasoning required in embodied settings to its simplest form. As such, the main applications of this work are in embodied AI, from VLN (Thomason et al., 2019) to cooperative task completion (Yang et al., 2025). While there are several intermediate steps before we can extend our findings to multimodal mod-

els, virtual tasks may benefit more directly. Take the MDC (Narayan-Chen et al., 2019), in which two agents collaborate to build a block-based structure in a 3D grid. Existing approaches struggle with shifting spatial reference frames caused by agents moving around the environment during the course of building (and thus might benefit from methods that improve performance on our *Egocentric Navigation* task). The *Object Localization* task addresses the issue of generating spatial relations for blocks relative to existing structures while the *Structure Composition* aligns with the MDC Architect describing a target structure, a part of the task that remains largely unexplored as recent work has focused on the instruction-following Builder (Jayannavar et al., 2025).

Our focus on smaller or unimodal models is further motivated by the practical constraints of real-world embodied AI, where the latencies of frontier models can significantly hinder a physical agent (Park et al., 2026; Pollini et al., 2025), hardware constraints may require lightweight models that can be fully housed inside a small robot, privacy concerns may necessitate local models or eschewing multimodal inputs at times (Marchang and Di Nuovo, 2022; Moncrieff et al., 2008), and specialized tasks may need further training anyway.

6 Conclusion

In this work, we propose GSU, a novel evaluation framework providing a controlled environment to test spatial reasoning and spatial communication without confounding factors like visual perception. Evaluating a variety of models, we found that most, even some frontier models, struggle to track rotating frames of spatial reference and understand how blocks at grid coordinates may be composed into structures, though recent models are crossing this threshold of spatial understanding. We also provide empirical evidence that exposure to a visual modality does not inherently guarantee improved spatial reasoning, or at least, communication about it, especially in smaller models, which goes against the current assumptions about VLM capabilities and raises questions about how the parametric knowledge gained from the modality is stored and accessed by models. Finally, we show that training lightweight models and small LLMs can match or outperform massive foundation models on these textual grid spatial reasoning tasks, supporting their use as specialized embodied agents.

Limitations

This work is, in part, limited by the nature of the proposed tasks. While the simplicity allows for extremely controlled observations on understanding, it is noted that such tasks may not directly generalize to real world settings outside of virtual environments. In particular, embodied scenarios that involve continuous space, visual noise, and partial observability, are not easily represented in the current formulation of GSU. That being said, we think generalizing to continuous space on a grid should be quite feasible, as math is not generally the feature that models struggle the most with. However, having more angles of rotation available to models in *Navigation* tasks will certainly increase the difficulty movement would no longer be nicely axes aligned (though arguable with the egocentric setting the most challenging component is keeping track of headings). In the future, it would be interesting to expand textual problems to incorporate partial observability, exploring if models can tell what would be in their line of sight and reasoning about what may be obscured. It might also present a means of checking information stored during exploration, creating more interesting problems such as reconciling information gathered from different viewpoints (that may not be expressed relative to the same overarching fixed grid). The most direction extension of grid coordinates into more physical problems would likely be in pointclouds and we would be interested to see if our findings generalize to those richer, longer contexts.

Within the confines of the task, we think there is room to further improve smaller models on GSU, explore possibilities such as using performance on a *Follower* task with more direct signal to improve *Instructor* performance, and see if forcing models to communicate about and reason over textual grids can force stronger internal representations or help connect parametric knowledge to visual information in multimodal models.

Acknowledgments

This work used the Delta system at the National Center for Supercomputing Applications through allocation CIS240333 from the Advanced Cyberinfrastructure Coordination Ecosystem: Services & Support (ACCESS) program, which is supported by National Science Foundation grants #2138259, #2138286, #2138307, #2137603, and #2138296.

All models were used within their licensing

agreements described on Huggingface. We thank the Mistral team for access to Mistral-7b and Pixtral, the Llama team for access to Llama-8b and Llama-11b-VL, the Qwen teams for access to Qwen-7b, Qwen-7b-VL, and Qwen-72b, AI2 for access to Olmo-32b, OpenAI for access to GPT-4o and GPT-OSS-20b, and Google for access to Gemini 3 Pro.

References

- Mohamed Aghzal, Erion Plaku, and Ziyu Yao. 2025. [Can large language models be good path planners? a benchmark and investigation on spatial-temporal reasoning](#). *Preprint*, arXiv:2310.03249.
- Pravesh Agrawal, Szymon Antoniak, Emma Bou Hanna, Baptiste Bout, Devendra Chaplot, Jessica Chudnovsky, Diogo Costa, Baudouin De Monicault, Saurabh Garg, Theophile Gervet, Soham Ghosh, Amélie Héliou, Paul Jacob, Albert Q. Jiang, Kartik Khandelwal, Timothée Lacroix, Guillaume Lample, Diego Las Casas, Thibaut Lavril, and 23 others. 2024. [Pixtral 12b](#). *Preprint*, arXiv:2410.07073.
- Janice Ahn, Rishu Verma, Renze Lou, Di Liu, Rui Zhang, and Wenpeng Yin. 2024. [Large language models for mathematical reasoning: Progresses and challenges](#). *Preprint*, arXiv:2402.00157.
- Jinze Bai, Shuai Bai, Shusheng Yang, Shijie Wang, Sinan Tan, Peng Wang, Junyang Lin, Chang Zhou, and Jingren Zhou. 2023. [Qwen-vl: A versatile vision-language model for understanding, localization, text reading, and beyond](#). *arXiv preprint arXiv:2308.12966*.
- Boyuan Chen, Zhuo Xu, Sean Kirmani, Brian Ichter, Danny Driess, Pete Florence, Dorsa Sadigh, Leonidas Guibas, and Fei Xia. 2024. [Spatialvlm: Endowing vision-language models with spatial reasoning capabilities](#). *Preprint*, arXiv:2401.12168.
- Jiaqi Chen, Tong Li, Jinghui Qin, Pan Lu, Liang Lin, Chongyu Chen, and Xiaodan Liang. 2022. [Uni-geo: Unifying geometry logical reasoning via reformulating mathematical expression](#). *Preprint*, arXiv:2212.02746.
- An-Chieh Cheng, Hongxu Yin, Yang Fu, Qiushan Guo, Ruihan Yang, Jan Kautz, Xiaolong Wang, and Sifei Liu. 2024. [Spatialrgpt: Grounded spatial reasoning in vision language models](#). *Preprint*, arXiv:2406.01584.
- Hyung Won Chung, Le Hou, Shayne Longpre, Barret Zoph, Yi Tay, William Fedus, Eric Li, Xuezhi Wang, Mostafa Dehghani, Siddhartha Brahma, Albert Webson, Shixiang Shane Gu, Zhuyun Dai, Mirac Suzgun, Xinyun Chen, Aakanksha Chowdhery, Sharan Narang, Gaurav Mishra, Adams Yu, and 12 others. 2022. [Scaling instruction-finetuned language models](#). *arXiv preprint*.

- Tongtong Feng, Xin Wang, Yu-Gang Jiang, and Wenwu Zhu. 2025. [Embodied ai: From llms to world models](#). *Preprint*, arXiv:2509.20021.
- Rao Fu, Jingyu Liu, Xilun Chen, Yixin Nie, and Wenhan Xiong. 2024a. [Scene-llm: Extending language model for 3d visual understanding and reasoning](#). *Preprint*, arXiv:2403.11401.
- Xingyu Fu, Yushi Hu, Bangzheng Li, Yu Feng, Haoyu Wang, Xudong Lin, Dan Roth, Noah A. Smith, Wei-Chiu Ma, and Ranjay Krishna. 2024b. [Blink: Multi-modal large language models can see but not perceive](#). *Preprint*, arXiv:2404.12390.
- Jiahui Gao, Renjie Pi, Jipeng Zhang, Jiacheng Ye, Wan-jun Zhong, Yufei Wang, Lanqing Hong, Jianhua Han, Hang Xu, Zhenguo Li, and Lingpeng Kong. 2025. [G-llava: Solving geometric problem with multi-modal large language model](#). *Preprint*, arXiv:2312.11370.
- Aaron Grattafiori, Abhimanyu Dubey, Abhinav Jauhri, Abhinav Pandey, Abhishek Kadian, Ahmad Al-Dahle, Aiesha Letman, Akhil Mathur, Alan Schelten, Alex Vaughan, Amy Yang, Angela Fan, Anirudh Goyal, Anthony Hartshorn, Aobo Yang, Archi Mitra, Archie Sravankumar, Artem Korenev, Arthur Hinsvark, and 542 others. 2024. [The llama 3 herd of models](#). *Preprint*, arXiv:2407.21783.
- Dan Hendrycks, Collin Burns, Saurav Kadavath, Akul Arora, Steven Basart, Eric Tang, Dawn Song, and Jacob Steinhardt. 2021. [Measuring mathematical problem solving with the math dataset](#). *Preprint*, arXiv:2103.03874.
- Yining Hong, Haoyu Zhen, Peihao Chen, Shuhong Zheng, Yilun Du, Zhenfang Chen, and Chuang Gan. 2023. [3d-llm: Injecting the 3d world into large language models](#). *Preprint*, arXiv:2307.12981.
- Prashant Jayannavar, Liliang Ren, Marisa Hudspeth, Risham Sidhu, Charlotte Lambert, Ariel Cordes, Elizabeth Kaplan, Anjali Narayan-Chen, and Julia Hockenmaier. 2025. [Bap v2: An enhanced task framework for instruction following in minecraft dialogues](#). *Preprint*, arXiv:2501.10836.
- Albert Q. Jiang, Alexandre Sablayrolles, Arthur Mensch, Chris Bamford, Devendra Singh Chaplot, Diego de las Casas, Florian Bressand, Gianna Lengyel, Guillaume Lample, Lucile Saulnier, L  lio Renard Lavaud, Marie-Anne Lachaux, Pierre Stock, Teven Le Scao, Thibaut Lavril, Thomas Wang, Timoth  e Lacroix, and William El Sayed. 2023. [Mistral 7b](#). *Preprint*, arXiv:2310.06825.
- Chengzu Li, Caiqi Zhang, Han Zhou, Nigel Collier, Anna Korhonen, and Ivan Vuli  . 2024a. [Topviewrs: Vision-language models as top-view spatial reasoners](#). *Preprint*, arXiv:2406.02537.
- Fangjun Li, David C. Hogg, and Anthony G. Cohn. 2024b. [Advancing spatial reasoning in large language models: An in-depth evaluation and enhancement using the stepgame benchmark](#). *Preprint*, arXiv:2401.03991.
- Yuan-Hong Liao, Rafid Mahmood, Sanja Fidler, and David Acuna. 2024. [Reasoning paths with reference objects elicit quantitative spatial reasoning in large vision-language models](#). *Preprint*, arXiv:2409.09788.
- Fangyu Liu, Guy Emerson, and Nigel Collier. 2023. [Visual spatial reasoning](#). *Preprint*, arXiv:2205.00363.
- Arjun Majumdar, Anurag Ajay, Xiaohan Zhang, Pranav Putta, Sriram Yenamandra, Mikael Henaff, Sneha Silwal, Paul Mccvay, Oleksandr Maksymets, Sergio Arnaud, Karmesh Yadav, Qiyang Li, Ben Newman, Mohit Sharma, Vincent Berges, Shiqi Zhang, Pulkit Agrawal, Yonatan Bisk, Dhruv Batra, and 5 others. 2024. [Openeqa: Embodied question answering in the era of foundation models](#). In *2024 IEEE/CVF Conference on Computer Vision and Pattern Recognition (CVPR)*, pages 16488–16498.
- Jims Marchang and Alessandro Di Nuovo. 2022. [Assistive multimodal robotic system \(amrsys\): security and privacy issues, challenges, and possible solutions](#). *Applied Sciences*, 12(4):2174.
- Julius Mayer, Mohamad Ballout, Serwan Jassim, Farbod Nosrat Nezami, and Elia Bruni. 2025. [ivispar – an interactive visual-spatial reasoning benchmark for vlms](#). *Preprint*, arXiv:2502.03214.
- Ida Momennejad, Hosein Hasanbeig, Felipe Vieira, Hiteshi Sharma, Robert Osazuwa Ness, Nebojsa Jojic, Hamid Palangi, and Jonathan Larson. 2023. [Evaluating cognitive maps and planning in large language models with cogeval](#). *Preprint*, arXiv:2309.15129.
- Simon Moncrieff, Svetha Venkatesh, and Geoff West. 2008. [Dynamic privacy assessment in a smart house environment using multimodal sensing](#). *ACM Trans. Multimedia Comput. Commun. Appl.*, 5(2).
- Anjali Narayan-Chen, Prashant Jayannavar, and Julia Hockenmaier. 2019. [Collaborative dialogue in Minecraft](#). In *Proceedings of the 57th Annual Meeting of the Association for Computational Linguistics*, pages 5405–5415, Florence, Italy. Association for Computational Linguistics.
- Team Olmo, :, Allyson Ettinger, Amanda Bertsch, Bailey Kuehl, David Graham, David Heineman, Dirk Groeneveld, Faeze Brahman, Finbarr Timbers, Hamish Ivison, Jacob Morrison, Jake Poznanski, Kyle Lo, Luca Soldaini, Matt Jordan, Mayee Chen, Michael Noukhovitch, Nathan Lambert, and 50 others. 2025. [Olmo 3](#). *Preprint*, arXiv:2512.13961.
- OpenAI. 2025. [gpt-oss-120b & gpt-oss-20b model card](#). *Preprint*, arXiv:2508.10925.
- OpenAI, Josh Achiam, Steven Adler, Sandhini Agarwal, Lama Ahmad, Ilge Akkaya, Florencia Leoni Aleman, Diogo Almeida, Janko Altschmidt, Sam Altman, Shyamal Anadkat, Red Avila, Igor Babuschkin, Suchir Balaji, Valerie Balcom, Paul Baltescu, Haiming Bao, Mohammad Bavarian, Jeff Belgum, and 262 others. 2024. [Gpt-4 technical report](#). *Preprint*, arXiv:2303.08774.

- Aishwarya Padmakumar, Jesse Thomason, Ayush Shrivastava, Patrick Lange, Anjali Narayan-Chen, Spananda Gella, Robinson Piramuthu, Gokhan Tur, and Dilek Hakkani-Tur. 2021. [Teach: Task-driven embodied agents that chat](#). *Preprint*, arXiv:2110.00534.
- Gyeongmuk Park, Seonghyeon Lee, and Yeonsu Park. 2026. [Minimizing response latency in llm-based agent systems: A comprehensive survey](#). *IEEE Access*, 14:26140–26168.
- Diego Pollini, Bruna V. Guterres, Rodrigo S. Guerra, and Ricardo B. Grandó. 2025. [Reducing latency in llm-based natural language commands processing for robot navigation](#). *Preprint*, arXiv:2506.00075.
- Zhihong Shao, Peiyi Wang, Qihao Zhu, Runxin Xu, Junxiao Song, Xiao Bi, Haowei Zhang, Mingchuan Zhang, Y. K. Li, Y. Wu, and Daya Guo. 2024. [Deepseekmath: Pushing the limits of mathematical reasoning in open language models](#). *Preprint*, arXiv:2402.03300.
- Zhengxiang Shi, Qiang Zhang, and Aldo Lipani. 2022. [Stepgame: A new benchmark for robust multi-hop spatial reasoning in texts](#). *Preprint*, arXiv:2204.08292.
- Mohit Shridhar, Jesse Thomason, Daniel Gordon, Yonatan Bisk, Winson Han, Roozbeh Mottaghi, Luke Zettlemoyer, and Dieter Fox. 2020. [Alfred: A benchmark for interpreting grounded instructions for everyday tasks](#). *Preprint*, arXiv:1912.01734.
- Ilias Stogiannidis, Steven McDonagh, and Sotirios A. Tsafaris. 2025. [Mind the gap: Benchmarking spatial reasoning in vision-language models](#). *Preprint*, arXiv:2503.19707.
- Yihong Tang, Ao Qu, Zhaokai Wang, Dingyi Zhuang, Zhaofeng Wu, Wei Ma, Shenhao Wang, Yunhan Zheng, Zhan Zhao, and Jinhua Zhao. 2025. [Sparkle: Mastering basic spatial capabilities in vision language models elicits generalization to spatial reasoning](#). *Preprint*, arXiv:2410.16162.
- Gemini Team, Rohan Anil, Sebastian Borgeaud, Jean-Baptiste Alayrac, Jiahui Yu, Radu Soricut, Johan Schalkwyk, Andrew M. Dai, Anja Hauth, Katie Millican, David Silver, Melvin Johnson, Ioannis Antonoglou, Julian Schrittwieser, Amelia Glaese, Jilin Chen, Emily Pitler, Timothy Lillicrap, Angeliki Lazaridou, and 1332 others. 2025. [Gemini: A family of highly capable multimodal models](#). *Preprint*, arXiv:2312.11805.
- Qwen Team. 2024. [Qwen2.5: A party of foundation models](#).
- Qwen Team. 2025a. [Qwen2.5-vl](#).
- Qwen Team. 2025b. [Qwen3 technical report](#). *Preprint*, arXiv:2505.09388.
- Jesse Thomason, Michael Murray, Maya Cakmak, and Luke Zettlemoyer. 2019. [Vision-and-dialog navigation](#). *Preprint*, arXiv:1907.04957.
- Jiayu Wang, Yifei Ming, Zhenmei Shi, Vibhav Vineet, Xin Wang, Yixuan Li, and Neel Joshi. 2024a. [Is a picture worth a thousand words? delving into spatial reasoning for vision language models](#). *Preprint*, arXiv:2406.14852.
- Peng Wang, Shuai Bai, Sinan Tan, Shijie Wang, Zhihao Fan, Jinze Bai, Keqin Chen, Xuejing Liu, Jialin Wang, Wenbin Ge, Yang Fan, Kai Dang, Mengfei Du, Xuancheng Ren, Rui Men, Dayiheng Liu, Chang Zhou, Jingren Zhou, and Junyang Lin. 2024b. [Qwen2-vl: Enhancing vision-language model’s perception of the world at any resolution](#). *arXiv preprint arXiv:2409.12191*.
- Ruonan Wang, Runxi Wang, Yunwen Shen, Chengfeng Wu, Qinglin Zhou, and Rohitash Chandra. 2025. [Evaluation of llms for mathematical problem solving](#). *Preprint*, arXiv:2506.00309.
- Yutaro Yamada, Yihan Bao, Andrew K. Lampinen, Jungo Kasai, and Ilker Yildirim. 2024. [Evaluating spatial understanding of large language models](#). *Preprint*, arXiv:2310.14540.
- An Yang, Baosong Yang, Binyuan Hui, Bo Zheng, Bowen Yu, Chang Zhou, Chengpeng Li, Chengyuan Li, Dayiheng Liu, Fei Huang, Guanting Dong, Haoran Wei, Huan Lin, Jialong Tang, Jialin Wang, Jian Yang, Jianhong Tu, Jianwei Zhang, Jianxin Ma, and 40 others. 2024. [Qwen2 technical report](#). *arXiv preprint arXiv:2407.10671*.
- Rui Yang, Hanyang Chen, Junyu Zhang, Mark Zhao, Cheng Qian, Kangrui Wang, Qineng Wang, Teja Venkat Koripella, Marziyeh Movahedi, Manling Li, Heng Ji, Huan Zhang, and Tong Zhang. 2025. [Embodiedbench: Comprehensive benchmarking multi-modal large language models for vision-driven embodied agents](#). *Preprint*, arXiv:2502.09560.
- Yue Zhang, Ziqiao Ma, Jialu Li, Yanyuan Qiao, Zun Wang, Joyce Chai, Qi Wu, Mohit Bansal, and Parisa Kordjamshidi. 2024. [Vision-and-language navigation today and tomorrow: A survey in the era of foundation models](#). *Preprint*, arXiv:2407.07035.
- Yurui Zhao, Xiang Wang, Jiahong Liu, Irwin King, and Zhitao Huang. 2025. [Towards geometry problem solving in the large model era: A survey](#). *Preprint*, arXiv:2506.02690.

A Dataset Generation

As GSU is a synthetic dataset and will release generation instructions, some of these statistics may vary or be further adjusted to preference. All dataset statistics reported here are for the test set.

A.0.1 Navigation

To generate the Navigation task, we simulate a grid traversal by randomly generating steps lengths (e.g. how many spaces will be traveled) and randomly

choosing a direction from the available options (i.e. in 2d we pick from left/right/forward/back and in 3d we also consider up/down) and pair them together. Then a function determines the final coordinates reached given the list of $(direction, length)$ pairs and the mode (e.g. *Egocentric* or *Cardinal*). When evaluating the *Follower* role, we provide the $(direction, length)$ pairs in natural language and expect a final coordinate as in Figure 1. In the *Instructor* role, we provide intermediate coordinates along the path as shown in Appendix C. As the base dataset construction is simply $(direction, length)$ pairs, the generated datasets are as similar as possible to compare the effects of various settings. That is, the *Instructor* and *Follower* tasks explore the exact same grid traversals but with switched inputs and outputs.

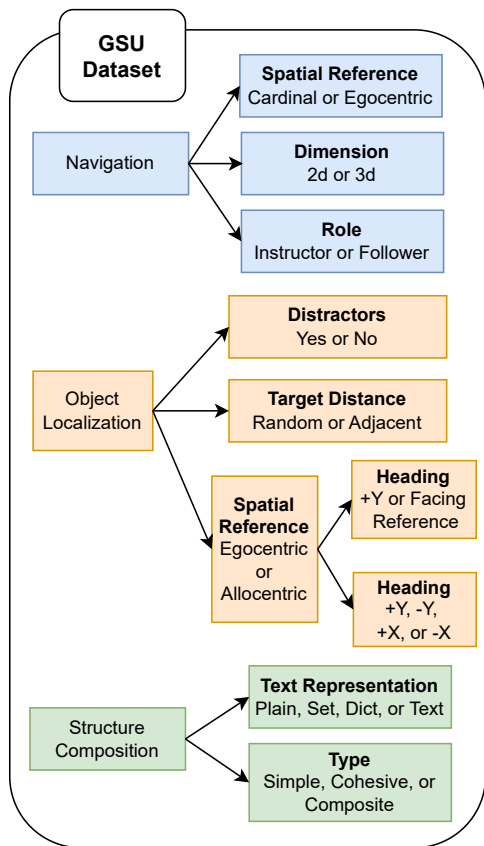


Figure 3: GSU Dataset Tasks and Settings

Path lengths are 1-4 steps, with 25% of each length, and an average path length of 2.5. Each step covers 1-10 units, averaging at 5.25. See 2 for the distribution of movements in each direction. We avoid having multiple steps in the same direction,

maximizing the direction changes that make the egocentric task difficult (in the 2D ego task, we change direction in 79.2% of transitions, in 3D, 49.8%, in cardinal 91%).

Table 2: Navigation Direction Distribution (reported out of 250 possible steps)

	Egocentric		Cardinal	
	2D	3D	2D	3D
Left	30.4%	17.69%	21.33%	16.67%
Right	29.6%	18.77%	34.67%	14.58%
Front	20.8%	13.72%	25.33%	12.5%
Back	19.2%	13.72%	18.67%	13.54%
Up	0	20.94%	0	29.17%
Down	0	15.16%	0	13.54%

A.0.2 Object Localization

For the *Egocentric* setting, we randomly sample 2 locations within the grid, which extends $(-20, 20)$ along all axes, designating one the target and one the reference/agent, and a heading along one of the horizontal axes $(+X, +Y, -X, -Y)$. For the adjacent case, we also sample one of the coordinates adjacent to the agent location (differing in each dimension by at most 1). In the *Allocentric* setting, we assume that the agent is at the origin and use the two sampled locations as the target and reference blocks. We set the heading either along the $+Y$ axis or towards the reference block.

For both settings, we select distractor blocks that do not overlap with the target block and programmatically derive the spatial relations.

Heading: In the Object Localization task, we can also vary the direction the embodied agent is facing. For the *Egocentric* setting, facing down a different axis greatly affects the spatial relations (e.g. a block that is in front of an agent facing the $+Y$ direction is to the right of an agent facing $-X$ as in 1). For the *Allocentric* setting, the agent may look in a fixed direction down the $+Y$ axis or directly at the reference object.

Target Distance: We choose if the target structures are placed adjacent to the spatial reference (i.e. adjacent to the agent in the *Egocentric* setting and adjacent to the reference block in the *Allocentric* setting) or anywhere on the grid, which is effectively further away due to how few coordinates are adjacent to a single coordinate. Unexpectedly, blocks that are directly adjacent to the reference location are harder for the model to describe spatially

(14). This trend was observed for the *Allocentric* setting as well, see 13.

We distribute targets across the grid w/ an average location: $(-0.44, 0.99, 0.44)$. In the adjacent *Egocentric OL* setting, the viewer and target are 1.37 apart on average, but may be 13.5 apart in the random setting. In the *Allocentric OL* variant, the target is on average 1.38 from the reference and 13.94 from the viewer (closest 2.4, furthest 22.5). For the ground truth answers, there are 1.96 and 1.98 directions per answer for the Ego and Allo variants respectively, with 2 directions being the most common (40% and 48% of all answers). However, 1 direction (32% and 27%) and 3 directions (28% and 25%) are also represented. Table 3 shows the distribution of each spatial direction in the ground truth answers.

	Egocentric	Allocentric
Left	18.88%	18.69%
Right	18.37%	13.64%
Forward	16.84%	17.17%
Backward	14.80%	6.57%
Up	20.41%	18.37%
Down	14.29%	13.64%

Table 3: Distribution of Ground Truth Spatial Direction in the Egocentric and Allocentric Object Localization settings

In our prompts (see Appendix E) we specify that all spatial relations should be given as *target* is $\langle spatial\ relations \rangle$ of *reference* and we found that nearly all generations followed this prescription. Thus, we found no need to account for the order of objects (i.e. in the *Egocentric* setting we assume all generations are relative to the agent, "the target is to the right of me", and ignore the possibility of "I am to the left of the target").

A.0.3 Structure Composition

To generate the Structure Composition task, we first generate 3 shapes and associated verbal descriptions using a template with minor variations for synonyms and grammatical structure. In the *Simple* setting we select the first shape and associated description, whereas in the *Cohesive* setting we then adjust half the blocks in the structure to be a different color and update the verbal description accordingly. Finally, for the *Composite* setting we translate the 3 shapes to be adjacent and join their textual descriptions with the appropriate spatial terms.

We initially explored a variety of textual representations for coordinates. In our *Plain* representation, coordinates are input into LLMs as sequences resembling pseudo-code:

$$\begin{aligned} &COLOR_1 X_1 Y_1 Z_1 \\ &\dots \\ &COLOR_N X_N Y_N Z_N \end{aligned}$$

We also explore alternate representations of coordinates, which this task is particularly suited for since it requires processing far more coordinates than previous tasks. The *Set* representation closely resembles *Plain*, but utilizes structures that the model might have encountered in code:

" $(COLOR_1, X_1, Y_1, Z_1), \dots, (COLOR_N, X_N, Y_N, Z_N)$ "

Dict resembles a dictionary where each value is explicitly labeled:

"(color = $COLOR_1$, x = X_1 , y = Y_1 , z = Z_1), ..., (color = $COLOR_N$, x = X_N , y = Y_N , z = Z_N)"

Text is a more verbal representation and the one used in the previous tasks:

"a $COLOR_1$ block at (X_1, Y_1, Z_1) , ..., and a $COLOR_N$ block at (X_N, Y_N, Z_N) ".

However, for brevity, we chose the overall best performing representation for the main paper, and include the supplementary results here (see 4). We found it interesting that, in general, the *Set* and *Text* representations were the best performing across all models (with notable exceptions, such as Qwen family models highly preferring the *Dict* representation), despite the convention in prior works to use the *Plain* formulation. We also anticipated the *Set* representation performing most similarly to the *Plain* as they were the most similar and were surprised to see that performance was quite different across these two settings. While the *Text* representation is not the most efficient, it follows that textual models would be able to best parse information presented in a form closer to natural language than to a set or dictionary.

For the generated block structures, examples have 2-199 blocks, with 61.77 on average. Looking further into the distribution shows a slightly right-skewed distribution, with 35% of structures having fewer than 15 blocks, and another 35% having between 15 and 85 blocks, and the remaining 40% of structures having 85+ blocks. We ensure that within the test set, we represent all 3 structure styles equally, one third being simple, one third being cohesive, and one third being composite. In terms of the other qualities, 49% of structures are

		Plain			Dict			Set		
		$O_s \uparrow$	$O_c \uparrow$	$O_f \uparrow$	$O_s \uparrow$	$O_c \uparrow$	$O_f \uparrow$	$O_s \uparrow$	$O_c \uparrow$	$O_f \uparrow$
0-shot	Mistral-7b	15.92	42.64	12.45	13.72	47.93	10.87	15.88	46.70	13.83
	Pixtral	37.67	74.36	14.64	44.67	70.13	13.62	32.08	72.91	7.25
	Llama-8b	21.29	63.90	13.00	22.78	63.91	15.56	25.47	68.83	18.65
	LlamaVL-11b	35.83	69.07	11.83	24.57	60.48	12.09	20.94	62.14	13.37
	Qwen-7b	32.17	68.72	11.48	40.03	68.32	16.73	28.52	62.76	16.65
	QwenVL-7b	18.21	60.37	8.08	33.47	52.78	12.81	30.32	45.83	11.62
1-shot	Mistral-7b	27.56	58.54	13.41	32.00	55.90	13.06	38.44	71.95	11.75
	Pixtral	64.58	82.49	24.20	63.00	81.98	20.22	64.20	89.59	31.18
	Llama-8b	59.90	63.37	17.81	55.83	66.74	20.83	59.70	85.83	30.19
	Llama-11b	63.83	64.75	22.54	59.50	79.86	16.40	60.33	88.96	27.35
	Qwen-7b	50.75	76.25	16.00	63.65	81.87	23.08	54.00	88.80	29.67
	Qwen-7b	52.52	65.72	8.24	55.67	62.57	13.38	66.90	85.27	23.37
Full FT	FlanT5	92.92	70.32	81.59	84.25	67.27	80.88	90.08	68.07	79.68

Table 4: Structure Composition results for Plain, Dict, and Set Representations

single color, a further 18% are two-colored, and 33% have 3 colors. We also have a fairly even distribution of numbers describing the structures, with most between 2-7, but a few outliers with 1 or 8-9. All structures were describable with numbers less than 10 (e.g. no columns or towers were more than 10 blocks high). Most structures could be described in 3 or less numbers, though for a few more might be needed (e.g. a structure with a tower flanked by 2 planes needs at least 6 numbers, more if you want to specify that the plane only has a width of one). Table 5 further gives the distributions of colors, spatial relations, and shapes.

A.1 Shape Metric

For the shape metric, we check for synonyms in the generation and map them to their corresponding shape. The synonyms are built around the base vocabulary and then appended to with common outputs in actual generations. For columns, we accept "column", as well any production with "vertical" or "upright" and "line" or "row". For rows, we accept any generation with "row" or "line" that does not mention verticality. For towers (multiple columns grouped together), we accept "tower", "rectangular prism", and "pillar". For planes (rectangular prisms only one block thick), we accept "plane", "platform", "rectangle", "wall", "square", "ring", and "O". For cubes, we accept "cube".

Furthermore, since shapes can be similar to others, if a generation does not match at least one of the ground truth shapes, we offer it partial credit

based on how similar the shape it predicted was. Confusing rows and columns leads 0.6 of the full 1.0 received for a total match, as does mixing up a column and a tower. Since towers and cubes are both rectangular prisms, we offer half credit for such mistakes, and 0.1 for towers and planes or planes and cubes, and 0.2 for rows and towers.

B Experimental Information

B.1 Training Details

For the LORA fine-tuning runs, we experimented with various ranks, learning rates, and training set sizes. Overall, we found that the model performance plateaued at its highest level with rank 64, a learning rate between $5e-4$ and $1e-5$ depending on the task, and a training set of size 3000. We used $\alpha=8$ as recommended in the original paper and an AdamW optimizer. We allowed the models to train for 4 epochs, but chose the model with the highest validation accuracy as the one to evaluate. For the FlanT5-large and BART-base runs, we allow the model to train for 15 epochs or until the loss converges using an AdamW optimizer with a learning rate of $5e-5$ for Flan and $1e-4$ for BART.

This project was run on up to 4 gpuA100x4's using approximately 1500 GPU hours of compute.

B.2 Ablations

Here we show another lightweight model (BART-base) and how both it and Flan-T5 perform before fine-tuning and after for Navigation (Table 6) and

Table 5: Distribution of Spatial Relations, Colors, and Shapes in the Structure Composition task

		Percentage
Spatial Relations	Above	19.67%
	Below	21.2%
	Front	19.67%
	Back	10.61%
	Left	12.12%
	Right	16.67%
Colors	Red	16.3%
	Orange	11.96%
	Yellow	21.73%
	Green	16.85%
	Blue	17.39%
	Purple	15.76%
Shapes	Cube	27.7%
	Tower	24.7%
	Row	19.88%
	Column	9.64%
	Plane	18.07%

Object Localization / Structure Composition (Table 7). We see that performance without any training is quite and improves a great deal for Flan-T5-Large, especially on sequence generation tasks in the *Navigation Instructor* in Table 6 and the *Structure Composition* task in Table 7. Since the smaller BART model does not improve as much, we do know that these results may not be generalizable to *all* LMs. Nevertheless, their size difference alone, merits acknowledgement that any LMs can perform comparably to frontier models.

C Model Selection

For the newer models used in the prompting experiments, we considered using the Thinking versions as they might be better suited to reasoning over grid logic, but found that the instruct models performed better. We also explored the Deepseek model distilled on Qwen32b, which received a 0.15 and a 0.26 on the *Egocentric Navigation Follower* task in 2D and 3D (compared to the 0.37 and 0.32 in the standard 32b model shown in 1). It also only received a 0.15 on the *Egocentric Navigation Instructor* task in 3D.

D Supplemental Results

D.1 Navigation

As expected, for the *Navigation Follower* task, we saw much stronger performance in the more predictable *Cardinal* setting (see Table 10), where even the smaller VLMs (Pixtral, Llama-11b-v, Qwen-7b-v) were consistently solving the 3D task (receiving scores of 0.67, 0.60, and 0.90, respectively), and were extremely proficient on the 2D task (with the LLama and Qwen models getting every example correct). Keeping track of how spatial relations changed with an embodied agents in the *Egocentric* posed a challenge even for GPT-4o and the largest tested Qwen model.

While the 3D *Cardinal* was more challenging than its 2D counterpart, we suspect that the higher scores in the 3D *Egocentric* setting are due to up/down movements not requiring turns by definition, which effectively shorted the number of rotations and led to fewer opportunities to introduce errors.

As explained in Section 3, we saw that giving one well-crafted example yielded a greater improvement in performance than several examples with just the ground truth answer. For the *Navigation* task, that is shown in Table 9, while the improvement against 0-shot prompting can be seen in Table 10

At the start of the generated reasoning traces, models seem to understand the standard Cartesian layout (when facing positive y, positive x is to your right), but as they progress through the instruction sequences they fail to keep this consistent with the actions they take. Sometimes, these incorrect justifications are followed by correct steps though, as in: "*we are facing negative x with positive x to the right [incorrect, +Y would be to the right] so that means that turning right means going towards positive x ... [rest of the step] ... now, we are facing positive y" [+Y being the correct axes to the right of -X, and thus the correct heading upon finishing the step].*

For the *Instructor* task, we see that performance is weaker than its *Follower* counterpart, but some models are still able to produce strong instruction sequences that get quite close to the desired endpoint, with Qwen-72b even solving the task completely. But the *Egocentric* setting again breaks what "understanding" these models possess, leading to performances well below a simple model of 875M parameters fully fine-tuned on the problem.

	Follower				Instructor					
	Egocentric 2D		Egocentric 3D		Cardinal		Egocentric		Card2Ego	
	acc \uparrow	dist. \downarrow								
Flan-T5 w/o finetune	0	34.64	0	28.28	0	8.79	0	7.82	0	8.23
Flan-T5 w/ finetune	0.3	4.21	0.71	1.68	0.99	0.02	0.9	0.42	1.0	0
BART w/o finetune	0	34.64	0	28.28	0	8.22	0	7.44	0	8.21
BART w/ finetune	0.24	2.37	0.09	7.82	0.26	2.72	0	6.29	0.85	1.37

Table 6: BART-base and Flan-T5-large Navigation Ablations

	Object Localization		Structure Composition			
	Egocentric	Allocentric	O_s	O_c	O_f	O_n
Flan-T5 w/o finetune	16.5	16.67	67	7.11	16.6	8.9
Flan-T5 w/ finetune	19.5	94.5	99	96.17	88.83	97.07

Table 7: BART-base and Flan-T5-Large Ablations over Object Localization and Structure Composition tasks

	Follower		Instructor		
	Egocentric 2D	Egocentric 3D	Cardinal	Egocentric	Card2Ego
Mistral-7b	6.85	6.14	2.84	11.87	11.23
Pixtral	6.31	5.60	0.75	7.65	9.01
Llama-8b	7.03	4.85	1.95	11.87	12.30
LlamaVL-11b	7.36	5.78	1.52	11.96	9.59
Qwen-7b	22.54	20.44	1.57	8.96	7.52
QwenVL-7b	7.9	12.91	4.54	7.46	7.74
GPT-oss-20b	17.67	13.95	5.76	11.35	4.95
Olmo-32b	7.22	5.94	4.59	8.20	4.24
Qwen-32b	6.37	12.71	3.14	8.80	4.08
QwenVL-32b	6.41	5.16	6.58	14.00	4.44
Qwen-72b	5.76	3.66	0.0	5.67	5.23
GPT-4o	2.94	1.40	0.56	4.04	0.77
Gemini-3-Pro	0.0	0.0	0.0	0.0	0.0
FlanT5	4.21	1.68	0.02	0.42	0.0
Llama-8b	1.59	0.17	2.58	2.31	0.21

Table 8: The distance off scores for each of the *Navigation* experiments in Table 1.

		Cardinal 3D		Egocentric 3D	
		acc	dist	acc	dist
1	Mistral-7b	0.48	4.14	0.38	6.14
	Llama-8b	0.62	2.65	0.47	4.85
	Qwen-7b	0.63	7.79	0.19	20.44
Few	Mistral-7b	0.19	6.23	0.17	8.32
	Llama-8b	0.32	4.84	0.20	7.69
	Qwen-7b	0.50	4.31	0.29	7.07

Table 9: 1-shot vs Few-shot Navigation: Comparison over 1-shot performance with reasoning vs Few-Shot without reasoning examples

Even Qwen-72b and GPT-4o, which show some promise on shorter sequences, get turned around in longer sequences.

To better understand the source of the errors in the *Egocentric* setting, we proposed the *Card2Ego* setting, which just required understanding how cardinal directions would change relative to an embodied traveller, removing the necessity of reasoning about specific coordinates and where they fall relative to each other. We found that models performed better in this setting, with medium sized models seeing notable improvements, but were still far from completely solving the task.

Looking at the reasoning traces generated in more detail, we saw that model accuracy dropped on paths with more steps, though this decrease was much more subtle in the cardinal task, occurring more often in weaker or fine-tuned models and due calculation errors / minor mistakes. For egocentric navigation, the dropoff in performance and corre-

		Follower								Instructor			
		Cardinal				Egocentric				Cardinal		Egocentric	
		2d		3d		2d		3d		2d	3d	2d	3d
		acc.↑	dist.↓	acc.↑	dist.↓	acc.↑	dist.↓	acc.↑	dist.↓	acc.↑	acc.↑	acc.↑	acc.↑
Mistral-7b	0.35	6.15	0.24	14.56	0.22	9.92	0.09	17.49	0.01	0.04	0.0	0.01	
Pixtral-12b	0.85	2.39	0.54	5.34	0.29	7.34	0.34	7.05	0.21	0.10	0.09	0.07	
Llama-8b	0.81	2.34	0.35	8.52	0.33	6.86	0.36	6.55	0.05	0.11	0.02	0.02	
LlamaVL-11b	0.80	2.28	0.37	9.20	0.28	7.55	0.38	6.13	0.06	0.10	0.03	0.04	
Qwen-7b	0.96	0.49	0.86	0.85	0.56	4.45	0.53	5.41	0.20	0.19	0.16	0.14	
QwenVL-7b	0.82	2.92	0.78	3.05	0.35	9.13	0.48	6.75	0.11	0.05	0.09	0.06	
Qwen-72b	-	-	0.67	2.40	-	-	0.36	6.21	-	0.62	-	0.37	
Mistral-7b	0.88	0.92	0.48	4.14	0.30	6.85	0.38	6.14	0.59	0.38	0.15	0.11	
Pixtral-12b	0.97	0.37	0.67	4.20	<u>0.33</u>	<u>6.31</u>	0.50	5.60	0.87	0.80	0.26	0.28	
Llama-8b	0.99	0.04	0.62	2.65	<u>0.33</u>	7.03	0.47	4.85	0.69	0.54	0.06	0.23	
LlamaVL-11b	1.00	0.0	0.60	2.94	0.32	7.36	0.47	5.78	0.74	0.59	0.14	0.21	
Qwen-7b	0.89	3.11	0.63	7.79	0.09	22.54	0.19	20.44	0.76	0.83	0.21	0.19	
QwenVL-7b	1.0	0.0	<u>0.90</u>	<u>1.02</u>	0.29	7.9	0.21	12.91	0.44	0.66	0.21	0.23	
Qwen-72b	-	-	1.00	0.00	-	-	<u>0.75</u>	3.66	-	0.99	-	<u>0.54</u>	
Full FT	FlanT5	-	-	0.94	0.09	-	-	0.82	13.14	-	0.90	-	0.85

Table 10: Navigation task results. We compare 0- and 1-shot prompting on base text-only LLMs, similarly sized VLMs (represented with light blue backgrounds), and a larger LLM variant of the overall best performing model, as well as a fully fine-tuned LM. We report the accuracies out of 1 for the final coordinates and their distance from the true coordinates for the *Follower* setting and the accuracy out of 1 of the generated instruction for the *Instructor* setting. The best results for each experiment are **bolded** while the best in each section are underlined.

Model Name	Sequence Length			
	1	2	3	4
Qwen-7b	1.0	0.24	0.08	0.08
Qwen-7b-v	0.92	0.2	0.04	0
Qwen-72b	1.0	0.56	0.28	0.12
Chat-GPT	1.0	0.72	0.68	0.44

Table 11: 2D Egocentric Follower Navigation Performance Deterioration Based on Sequence Length

sponding increase in the "distance off" metric were much sharper. Many of the weaker models went from accuracies in the 70s and 80s for shorter sequences to 0 or almost 0 in the longer sequences, but even strong models saw performance drops from almost perfect accuracy to numbers in the 60s and 70s.

Observing the reasoning traces produced by the models for the navigation tasks show that in addition to preferring shorter sequences, most models perform better on backward direction changes as opposed to right/left direction changes. Models were also more likely to produce incorrect conclusion in these longer sequences, particularly in the egocentric navigation tasks. Other times, models across families (GPT, Qwen, Llama) would correctly compute the new headings but not make use of them, falling back to the cardinal version of the problem. Or, they would twist the logic to make

the egocentric direction changes align with the direction in a cardinal setting. For example, when facing negative x: "Moving 8 steps back means moving opposite the direction we are facing. So we will move along positive x, i.e. increase the x value by 8. [consistent with facing the $-X$ direction] However, since we are facing negative x, we need to move along negative x, i.e. decrease the x value by 8. [the complete opposite] So, our new position is $(-3 - 8, 0) = (-11, 0)$. Since we turned to move, we are now facing negative x and positive y is to our right" (Llama-8b). This often led models to perform very well on shorter egocentric sequences where the error had not yet compounded, but rapidly diverge on longer sequences. We also found that models produced similar errors within their model family (e.g. Qwen-7b predicting the same incorrect coordinates as the 72B version or the vision version). Smaller models were also less internally consistent and likely to make mistakes about how axes were oriented relative to each other ("since we are facing positive x, negative y is to our left") or other errors (e.g. when moving 9 steps in one direction, incrementing all the x-, y-, z- values by 9). These errors were much less prevalent in the cardinal variants of these tasks, leading us to believe that basic math and reasoning are not the issue in these tasks, but rather keep the rotations / current heading state consistent with previous move and

keeping the axes consistent with each other.

D.2 Object Localization

For the *Egocentric* Object Localization task, we tested the models on the hardest setting (adjacent target blocks with additional distractors) and in various headings in a 3D grid and saw the expected pattern of improvement from larger models.

We further looked into accuracy based on the heading (see Table 12 in the Appendix for more), and found that models mostly performed best in the +Y heading that we would consider the "standard" for the Cartesian grid, with the Qwen family and our fine-tuned model showing the strongest preference (perhaps due to exposure to a similar environment or task in pre-training). For the other 3 headings there was no clear preference between all models, with some preferring the -Y heading as second best and others the headings parallel to the X-axis. We see the effects of this axis preference compounded in the *Egocentric* Navigation task, where models struggle to identify spatial directions in non-standard headings.

Especially in the smaller models, we saw a lack of understanding of how axes were situated relative to each other (similar to the Navigation task). We also observed confusion over whether the y or z axis was vertical (despite it being explicitly stated) leading to productions such as, "*the block is below and above me*". There were common incorrect conclusions such as, "*I am facing negative y so smaller values are in front of me. [correct] My y is -4 and the block's is 7, so it is **above** me*". In general, these mistaken deductions were aligned with a standard +Y heading rather than the correct premise preceding them, showing that despite any intermediate generations to the contrary, the models were still operating in that +Y heading.

	+Y	+X	-Y	-X
Mistral-7b	36.90	34.98	29.13	32.26
Llama-8b	51.33	40.23	43.80	37.84
Qwen-7b	77.27	52.10	38.26	44.32

Table 12: Average Spatial Overlaps O_s in the *Egocentric* Object Localization task broken down by Viewer Heading

For the *Allocentric* Object Localization task, we evaluated only on the +Y heading so the slight performance drops compared to the *Egocentric* formulation are actually much more pronounced con-

	+Y Heading		Facing Reference	
	adj	rand	adj	rand
0-shot	32.90	38.67	29.67	38.12
1-shot	46.50	39.83	32.32	41.75

Table 13: Adjacent vs Random Block placements in the *Allocentric* Object Localization Task for Mistral-7b

sidering that models perform best on this heading.

Looking at the errors made by models for *Egocentric* Object Localization, models that performed better tended to correctly identify how many dimensions differed between the target and viewer coordinates, thus producing the correct number of relative directions. However, poorer performing models tended to predict extra directions (e.g. claiming the target was to the front right of the viewer when it was directly to the right). Looking into these predicted directions, we saw that models were consistently getting up/down difference correct (which makes sense, given that the various headings never affected the z-axis), but tended to predict that objects were to the left when they were to the right, or add in extra above/below directions even when the objects were level with the viewer. The Qwen models had consistently higher performance for the +y heading but other models did not show as much preference. Within the reasoning traces, stronger models were able to break down the problem by each axis and emulate the example reasoning trace to properly using the given heading and surmise what the direction should be. Weaker models were more likely to fail to make a connection between the viewer's heading and the directions, break down the reason trace by axes but proceed as if always facing +y, incorrectly identify the vertical axis, and to make incorrect conclusions from correct premises (e.g. "same y value so the target is level and thus in front of the viewer").

For the *Allocentric* variant, models were more likely to produce fewer dimensions than the ground truth, and very often struggled with the front/back distinction shown in Figure 2. Models were mostly likely to extraneously add an incorrect left/right dimensions, and some models seemed to have a preference for which direction they incorrectly predicted (e.g. Qwen72b was more likely to predict left for a ground truth right, than predict right for a ground truth left). We generally saw very structured and consistent reasoning traces, but in the cases of those front/back examples the prompt

instructions/examples tended to be ignored in favor of some existing underlying understanding of front/back. Weaker models struggled to keep the axes oriented correctly (often leading to mixups with the vertical dimension) and sometimes referred to where the target was relative to the viewer rather than to the reference.

D.3 Structure Composition

We saw spatial results similar to the *Allocentric* ones, with just slight improvements in some models, likely due to the perspective difference in the task definition: in the *Allocentric* setup we treat the reference as having its own spatial reference (i.e. it has a left and right of its own, mirroring those of the viewer), whereas in the Structure Composition setup we defer to a viewer facing along the $+Y$ axis for spatial terms to preserve the simplicity of the task. This simpler spatial referencing is offset by the higher number of blocks and the need to group and then orient them correctly.

Naturally, the O_f subtask was the most difficult since it requires models to match groupings of coordinates to real-life shapes that exist outside of grid and coordinate settings, making the fully fine-tuned model’s performance all the more impressive. Reflective of the wide vocabulary that models might apply to these shapes, we used generous synonyms in the shape metric (see Appendix A.1). As such, an O_f score around 50, reflects a mastery of simple shapes like columns and rows in their individual and *Composite* settings and some limited success with more complex shapes such as towers, rectangular prisms, and cubes, whereas one near 90 suggests a mastery of individual shapes and composite structures, with occasional errors, usually on larger shapes. Finally, we did see shape preference in the model outputs, with certain models generally not predicting certain types of shapes (depending on the model, this was generally a cube or a tower).

We also show results for the various coordinate representation formats discussed in Section A.0.3 in Table 4 and the performance difference between more few-shot examples with no reasoning and a single 1-shot example with strong reasoning in Table 15.

		Egocentric				Allocentric	
		Base		Distractors		+Y heading	Ref. heading
		adj. \uparrow	rand. \uparrow	adj. \uparrow	rand. \uparrow	adj. \uparrow	adj. \uparrow
0-shot	Mistral-7b	30.87	34.67	30.20	31.90	32.90	29.67
	Pixtral-12b	35.22	42.54	31.42	46.73	40.73	34.43
	Llama-8b	36.52	38.78	37.08	33.10	37.11	35.52
	LlamaVL-11b	35.33	41.50	33.08	36.55	41.08	39.72
	Qwen-7b	<u>53.55</u>	<u>48.20</u>	<u>53.07</u>	<u>49.02</u>	<u>51.75</u>	<u>46.82</u>
	QwenVL-7b	26.18	37.83	31.98	36.15	46.75	43.25
	Mistral-7b	30.30	40.22	30.32	39.61	46.50	32.32
	Pixtral-12b	<u>57.55</u>	65.87	40.83	54.30	48.18	42.25
	Llama-8b	48.48	52.82	46.17	50.28	50.18	42.37
	LlamaVL-11b	53.56	58.27	48.40	51.55	48.08	48.20
	Qwen-7b	53.80	59.70	52.81	<u>55.42</u>	<u>54.78</u>	47.93
	QwenVL-7b	51.78	52.42	48.67	52.42	44.95	41.08
	QwenVL-72b	-	-	<u>79.53</u>	79.45	53.83	47.62
LORA	Mistral-7b	-	-	36.72	62.62	59.03	47.89
	Llama-8b	-	-	80.05	<u>72.60</u>	<u>61.58</u>	<u>84.03</u>
Full FT	FlanT5	98.08	65.75	73.03	62.50	100	96.1

Table 14: Object Localization spatial overlap, O_s , scores across the *Egocentric* and *Allocentric* settings, as well various headings and distractor settings. VLM counterparts are in light blue backgrounds, best results overall are **bolded** and best results in generation setting are underlined.

		Set			Text		
		$O_s \uparrow$	$O_c \uparrow$	$O_f \uparrow$	$O_s \uparrow$	$O_c \uparrow$	$O_f \uparrow$
1-shot	Mistral-7b	26.14	54.12	15.18	34.73	57.10	24.22
	Llama-8b	59.98	63.58	18.69	60.26	67.05	22.16
	Qwen-7b	54.70	74.86	20.85	57.18	71.78	19.14
Few-shot	Mistral-7b	38.44	71.95	11.75	49.75	72.60	26.33
	Llama-8b	59.70	85.83	30.19	62.04	86.69	26.10
	Qwen-7b	54.00	88.80	29.69	54.58	85.43	25.67

Table 15: 1-shot vs Few-shot Structure Composition: Comparison over 1-shot performance with reasoning vs Few-Shot without

E Prompt and Generation Examples

E.1 Instructor Navigation

2d Egocentric Navigation Instructor Prompt w/ 1-shot Example

You are in a 2D environment with (x, y) coordinates set up like a standard horizontal Cartesian plane. You will start at the origin $(0, 0)$, which is at the center of this grid. You are currently facing the positive y direction, with the positive x direction to your right. However, when you move in a direction you must turn to face that direction, rotating your frame of reference. For example, if you move left, you will rotate 90 degrees and be facing the negative x direction with positive y to your right.

First, let me give you an example! You start at $(0, 0)$, go to $(3, 0)$, go to $(3, 1)$, and end at $(3, -1)$. Describe the path that traverses the provided coordinates.

I must remember that each time I move left, right, or back, I will be turning to face a new direction.

1. To get from $(0, 0)$ to $(3, 0)$, I must move 3 steps to the right. I will now be facing the positive x direction, with negative y to my right.

2. To get from $(3, 0)$ to $(3, 1)$, I must move 1 step left. I will now be facing positive y , with positive x to my right.

3. To get from $(3, 1)$ to $(3, -1)$, I must move 2 steps back. So, my path is [ANS] right 3, left 1, back 2 [/ANS]. Great, now let's try a real problem!

Start at $(0, 0, 0)$. Go to $(0, 7, 0)$. Go to $(0, -1, 0)$. End at $(-4, -1, 0)$. Describe the path that you will take to traverse the provided coordinates. Format your answer as a series of directions and distances, e.g. [ANS] forward 2, right 3, back 1 [/ANS]. Let's go!

Mistral-7b Generation

CORRECT ANSWER : ['forward 7', 'backward 8', 'right 4']

GENERATED ANSWER : ['forward 7', 'backward 8', 'backward 4', 'forward 1']

2d Card2Ego Navigation Instructor Prompt w/ 1-shot Example

You are on a 2D grid and will be given a path using cardinal directions (North, East, South, West) that you need to convert into egocentric directions (left, right, forward, backward). Keep in mind that to move in a cardinal direction, you must turn to face it. This means that the egocentric instructions will not map directly to cardinal ones, but change depending on the direction you last moved. E.g. if you just moved East and then want to move South, then the egocentric instruction is to move right, since South is to your right if you're facing East.

Let's begin with an example. You start by facing North and the path is: West 2, North 3, East 1.

The first step is easy. I am facing North and must move West which is to my left. So the first step is: left 2.

Now, for the second step I am facing the direction I just moved in, West, and I want to move North.

If I am facing West, North is to my right. So the instruction is right 3.

Then, for the third step I am facing North and want to go East 1. East is to my right and so I need to move right 1.

Finally, I can put that all together for: [ANS] left 2, right 3, right 1 [/ANS] Now, you give it a try! You start facing North and the path is: West 3, East 8, South 1, South 10. What is the path expressed with egocentric directions?

GPT-4o Generation

CORRECT ANSWER : [left 3, backward 8, right 1, forward 10]

GENERATED ANSWER : Let's break it down step by step.

1. Start facing North. To go West means turning left. - Instruction: left 3
 2. Now facing West. To go East means turning around (backward). - Instruction: backward 8
 3. Now facing East. To go South means turning right. - Instruction: right 1
 4. Still facing South. To go South again means going forward. - Instruction: forward 10
- Putting it all together: [ANS] left 3, backward 8, right 1, forward 10 [/ANS]

E.2 Follower Navigation

3d Egocentric Navigation Follower Prompt w/ 1-shot Example

You are in a 3D environment with (x, y, z) coordinates set up like a standard Cartesian plane. The x and y dimensions are horizontal, while the z dimension is the vertical component. You will start at the origin $(0, 0, 0)$, which is at the center of this grid. You are currently facing the positive y direction, with the positive x direction to your right. However, when you move in a direction you must turn to face that direction, rotating your frame of reference. For example, if you move left, you will rotate 90 degrees and be facing the negative x direction with positive y to your right. Explain your final coordinates after travelling. Please format your final coordinates as: [ANS] (x, y, z) [/ANS]. Let's go!

Let's start with an example: First, you move 3 steps to your right. Next, you move 2 steps down. You move 4 steps backwards. Finally, you move 2 steps left. Where are you now?

To solve this, we should break down the steps we take.

1. We start at $(0, 0, 0)$ facing the positive y direction, with positive x to our right.
2. Moving 3 steps right means moving along positive x , i.e. increasing the x value by 3. So, our new position is $(3, 0, 0)$. Also, we turned to face positive x , so now negative y is to our right.
3. Moving 2 steps down means moving along negative z , i.e. decreasing the z value by 2. So, our new position is $(3, 0, -2)$. Remember that moving up and down doesn't change our heading, so we are still facing positive x with negative y to our right.
4. Moving 4 steps back means moving opposite the direction we are facing. So we will move along negative x , i.e. decrease the x value by 4. So, our new position is $(-1, 0, -2)$. Since we turned to move, we are now facing negative x and positive y is to our right.
5. Moving 2 steps left means moving away from the right. So we will move along negative y , i.e. decrease y by 2. So, our new position is $(-1, -2, -2)$. Our final position is [ANS] $(-1, -2, -2)$ [/ANS]

Now, let's try a real problem! First, you move 7 steps to your right. You then move 5 steps forward. You move 10 steps up. Lastly, you move 5 steps backward. Explain your final coordinates:

Mistral-7b Generation

Correct Answer is : 'x': 7, 'y': 0, 'z': 10

Generated Coordinates are : $(7, 0, 10)$

E.3 Egocentric Object Localization

3d Egocentric Object Localization w/ Distractors, 1-shot Example

You are in a 3D environment with (x, y, z) coordinates set up like a standard Cartesian plane. The x and y dimensions are horizontal, while the z dimension is the vertical component. All axes range from $(-10, 10)$. Your task is to describe where objects are relative to you, without using coordinates. Instead use relative descriptions like 'directly behind me' or 'to my left'. Explain your thought process and please format your final answer with [ANS] tags like so: the green block is [ANS] in front of me and to my left [/ANS]. Let's get started!

Here is an example: You are at $(2, 2, 0)$, facing the negative y direction, so negative x is to your right. The positive z axis is always up. There is a blue block at $(-3, -1, 0)$. Where is the blue block relative to you?

For the x dimension, I know that negative x is to my right. That means x values smaller than mine are to my right and ones bigger than mine are to my left. My x coordinate is 2 and the blue block's is -3. So it is to my right.

Next, for the y dimension, I know that I am facing negative y , so it is in front of me. This means that y values smaller than mine are in front of me and those bigger than mine are behind me. My y coordinate is 2 and the blue is at -1. So, it is in front of me.

Now, for the z dimension, my orientation does not matter. Higher z values are above me and lower z values are below me. However, we are both at $z = 0$, so we are level. Putting that together, the blue block is [ANS] to my right and slightly to the front [/ANS]

Now let's try a real problem! You are at $(-1, 5, -9)$, facing the negative y direction, so negative x is to your right. The positive z axis is always up. There is a yellow block at $(-2, -1, -3)$, a orange block at $(3, 2, -3)$, a green block at $(-1, 4, 10)$, a red block at $(-7, 1, 7)$, and a blue block at $(2, 9, -9)$. Where is the red block relative to you?

Generation by Qwen-7b

Correct Answer is : The red block is [ANS] in front of me, to my right, and above me [/ANS]

Generated Description is : The red block is [ANS] to my left and behind me [/ANS]

BLEU : 0.0

BERT : 0.8915

SPATIAL OVERLAP : 0.0

E.4 Allocentric Object Localization

3d Allocentric Object Localization w/ +Y heading, 1-shot Example

You are in a 3D environment with (x, y, z) coordinates set up like a standard Cartesian plane. The x and y dimensions are horizontal, while the z dimension is the vertical component. All axes range from $(-20, 20)$. Your task is to describe where objects are relative to you and other objects, without using coordinates. Instead use relative descriptions like 'directly in front of the blue cylinder'. Explain your thought process and please format your final answer with [ANS] tags like so: the yellow block is [ANS] below and to the back right of [/ANS] the purple block. Let's get started! You are at the origin. There is a red block at $(0, 8, -7)$ and a blue block at $(0, 7, -8)$. You may assume that you are facing the positive y direction. The positive z axis is always up. Where is the blue block relative to the red block given your point of view?

Llama-8b Generation

Correct Answer is : The red block is [ANS] below and in front of [/ANS] the blue block.

Generated Description is : The red block is [ANS] below and to the back of [/ANS] the blue block.

BLEU : 0.0

BERT : 0.826

SPATIAL OVERLAP : 0.33

E.5 Composite Description

Composite Structure Composition Task

You are in a 3D grid environment with (x, y, z) coordinates set up like a standard Cartesian plane. The x and y dimensions are horizontal, while the z dimension is the vertical component. Your task is to describe a set of blocks to someone without mentioning coordinates or axes, instead describe the structures as a whole. Format your answer with [ANS] tags like so: there are [ANS] 6 orange blocks in a column [/ANS].

Blocks: The blocks placed on the grid are: (color : purple, x : 0, y : 0, z : 0), (color : purple, x : 0, y : 0, z : 1), (color : purple, x : 0, y : 0, z : 2), (color : purple, x : 0, y : 0, z : 3), (color : purple, x : 0, y : 0, z : 4), (color : purple, x : 0, y : 0, z : 5), (color : purple, x : 0, y : 0, z : 6), (color : purple, x : 0, y : 0, z : 7), (color : purple, x : 0, y : 1, z : 0), (color : purple, x : 0, y : 1, z : 1), (color : purple, x : 0, y : 1, z : 2), (color : purple, x : 0, y : 1, z : 3), (color : purple, x : 0, y : 1, z : 4), (color : purple, x : 0, y : 1, z : 5), (color : purple, x : 0, y : 1, z : 6), (color : purple, x : 0, y : 1, z : 7), (color : purple, x : 1, y : 0, z : 0), (color : purple, x : 1, y : 0, z : 1), (color : purple, x : 1, y : 0, z : 2), (color : purple, x : 1, y : 0, z : 3), (color : purple, x : 1, y : 0, z : 4), (color : purple, x : 1, y : 0, z : 5), (color : purple, x : 1, y : 0, z : 6), (color : purple, x : 1, y : 0, z : 7), (color : purple, x : 1, y : 1, z : 0), (color : purple, x : 1, y : 1, z : 1), (color : purple, x : 1, y : 1, z : 2), (color : purple, x : 1, y : 1, z : 3), (color : purple, x : 1, y : 1, z : 4), (color : purple, x : 1, y : 1, z : 5), (color : purple, x : 1, y : 1, z : 6), (color : purple, x : 1, y : 1, z : 7), (color : yellow, x : 0, y : -2, z : 0), (color : yellow, x : 0, y : -2, z : 1), (color : yellow, x : 0, y : -2, z : 2), (color : yellow, x : 0, y : -2, z : 3), (color : yellow, x : 0, y : -2, z : 4), (color : yellow, x : 0, y : -1, z : 0), (color : yellow, x : 0, y : -1, z : 1), (color : yellow, x : 0, y : -1, z : 2), (color : yellow, x : 0, y : -1, z : 3), (color : yellow, x : 0, y : -1, z : 4), (color : yellow, x : 1, y : -2, z : 0), (color : yellow, x : 1, y : -2, z : 1), (color : yellow, x : 1, y : -2, z : 2), (color : yellow, x : 1, y : -2, z : 3), (color : yellow, x : 1, y : -2, z : 4), (color : yellow, x : 1, y : -1, z : 0), (color : yellow, x : 1, y : -1, z : 1), (color : yellow, x : 1, y : -1, z : 2), (color : yellow, x : 1, y : -1, z : 3), (color : yellow, x : 1, y : -1, z : 4), (color : red, x : 0, y : 0, z : 8), (color : red, x : 0, y : 1, z : 8), (color : red, x : 0, y : 2, z : 8), (color : red, x : 0, y : 3, z : 8), (color : red, x : 0, y : 4, z : 8), (color : red, x : 1, y : 0, z : 8), (color : red, x : 1, y : 4, z : 8), (color : red, x : 2, y : 0, z : 8), (color : red, x : 2, y : 4, z : 8), (color : red, x : 3, y : 0, z : 8), (color : red, x : 3, y : 1, z : 8), (color : red, x : 3, y : 2, z : 8), (color : red, x : 3, y : 3, z : 8), (color : red, x : 3, y : 4, z : 8) Now describe the structure they made.

Qwen-7b Generation

Correct Answer is : 8 x 2 x 2 purple tower with a tower of yellow blocks 5 high and 2 wide in front of it and a empty 4 x 5 red wall above it

Generated Description is : two large purple platforms stacked on top of each other, both extending from the bottom to the top of the visible area, and a smaller yellow platform that extends from slightly below the bottom to just above the middle of the visible area. Additionally, there is a red block formation at the very top, creating a cross-like pattern centered around the central vertical axis

BLEU : 0.0

BERT : 0.8357

SPATIAL OVERLAP : 0.2

COLOR OVERLAP : 1.0

SHAPE OVERLAP : 0.4

NUMERICAL OVERLAP : 0.0

E.6 Combination Task

Combination Navigation and Structure Localization Task

You are in a 3D environment with (x, y, z) coordinates set up like a standard Cartesian plane. The x and y dimensions are horizontal, while the z dimension is the vertical component. You are at the origin (0, 0, 0), which is at the center of this grid, facing the positive y direction, with the positive x direction to your right. However, when you move in a direction you must turn to face that direction, rotating your frame of reference. For example, if you move left, you will rotate 90 degrees counterclockwise and be facing the negative x direction with positive y to your right. There is a red block at (-10, 9, -5), **[excluded for human readability]** and a red block at (-12, 11, -4). You move 5 steps to your right. You then move 10 steps backward. You move 5 steps to your left. You also move 2 steps to your left. Next, you move 3 steps backward. You move 3 steps forward as well. Next, you move 1 step backward. Finally, you move 6 steps to your left. Now, where is the row relative to the plane given your point of view?

Gemini Generation

To determine the position of the row relative to the plane from your point of view, we first need to trace your movements to find your final position and facing direction.

1. Tracing Your Movements:

* **Initial State:** You start at '(0, 0, 0)' facing the positive y-direction (+y). Positive x (+x) is to your right.

* **Move 5 steps to your right:** You turn to face +x and move 5 steps.

* **Position:** '(5, 0, 0)' | *Facing:* +x

* **Move 10 steps backward:** "Backward" from +x is -x. You turn to face -x and move 10 steps.

* **Position:** '(-5, 0, 0)' | *Facing:* -x

* **Move 5 steps to your left:** Left of -x is -y. You turn to face -y and move 5 steps.

* **Position:** '(-5, -5, 0)' | *Facing:* -y

* **Move 2 steps to your left:** Left of -y is +x. You turn to face +x and move 2 steps.

* **Position:** '(-3, -5, 0)' | *Facing:* +x

* **Move 3 steps backward:** Backward from +x is -x. You turn to face -x and move 3 steps.

* **Position:** '(-6, -5, 0)' | *Facing:* -x

* **Move 3 steps forward as well:** "Forward" means you continue moving in your currently facing direction (-x).

* **Position:** '(-9, -5, 0)' | *Facing:* -x

* **Move 1 step backward:** Backward from -x is +x. You turn to face +x and move 1 step.

* **Position:** '(-8, -5, 0)' | *Facing:* +x

* **Move 6 steps to your left:** Left of +x is +y. You turn to face +y and move 6 steps.

* **Position:** '(-8, 1, 0)' | *Facing:* +y

* **Your Final State:** You are at **(-8, 1, 0)** facing the positive y-direction (**+y**). From your perspective:

* **Forward:** +y direction

* **Right:** +x direction

* **Up:** +z direction

2. Locating the Structures:

By analyzing the coordinates of the blocks, we can identify the specific grouped structures:

* **The Plane (Frame):** There is a hollow rectangular plane of blocks situated exactly at 'z = 8'.

It spans 'x = 0' to '5' and 'y = 7' to '13'.

* **Center of the Plane:** '(2.5, 10, 8)'

* **The Row:** There is a horizontal line of 7 blocks that spans entirely along the x-axis from 'x = -3' to '3'.

* **Center of the Row:** '(0, 8, -5)'

3. Determining Relative Position from Your Perspective:

Now, we compare the center of the Row '(0, 8, -5)' to the center of the Plane '(2.5, 10, 8)' relative to your point of view facing +y.

* **Left/Right (x-axis):** The row's center 'x = 0' is less than the plane's center 'x = 2.5'. Since +x is your right, a smaller x coordinate means it is to the **left**.

* **Front/Behind (y-axis):** The row's center 'y = 8' is closer to your position at 'y = 1' than the plane's center at 'y = 10'. Because you are facing +y, objects with a smaller y-value are closer to you, placing the row **in front of** the plane.

* **Above/Below (z-axis):** The row is at 'z = -5' while the plane is up at 'z = 8'. Since your up is +z, the row is vertically **below** the plane.

* **Conclusion:**

Given your point of view, the row is located to the **left, in front of, and below** the plane.

SPATIAL OVERLAP : 1.0